Journal of Applied Fluid Mechanics, Vol. 16, No. 9, pp. 1828-1838, 2023.
Available online at www.jafmonline.net, ISSN 1735-3572, EISSN 1735-3645.
https://doi.org/10.47176/jafm.16.09.1735

Characteristics of Olive Oil Droplet Combustion with Various Temperatures and Directions of Magnetic Fields in the Combustion Chamber

D. Perdana†, M. Hanifudin, M. K. Rosidin and W. A. Winarko

Department of Mechanical Engineering, Maarif Hasyim Latief University, Sidoarjo, East Java, 61257, Indonesia

†*Corresponding Author Email: dony_perdana@dosen.umaha.ac.id*

ABSTRACT

This study examines the effects of temperatures and directions of the magnetic fields in the combustion chambers on flame characteristics for boiler combustion in power generation systems by burning olive oil droplets. The variations in the temperature of the combustion chamber are 40°C, 50°C, and 60°C. Meanwhile, the directions of the magnetic fields are the repulsive magnetic field (north-north) and the attractive magnetic field (north-south). In the experiment, a droplet of olive oil was placed at a type K thermocouple junction between the two bar magnets. A 250 fps high-speed camera recorded the flame from its ignition to its extinction. The results of this study found that temperature and direction of the magnetic fields in the combustion chamber have an effect on the characteristics of the flame, where the attractive magnetic field (north-south) resulted in increased burning of droplets, round flame, low altitude, increased temperature, and shorter ignition delay time, compared to the repulsive magnetic field (north-north) and without a magnetic field. Furthermore, the combustion chamber temperatures of 40°C, 50°C, and 60°C produced flame temperatures of 799.94°C, 829.25°C, and 879.50°C, and flame heights of 5.97 mm, 5.35 mm, and 4.23 mm, respectively. The strong magnetic fields increased the concentration of oxygen and fuel molecules around the combustion reaction zone, causing shorter droplet combustion and releasing a large amount of energy. These findings are beneficial for designing efficient industrial heat generators with a magnetic field. The results of this study are therefore crucial as a basis for considering the substitution of fossil fuels with environmentally friendly vegetable oils.

Article History

Received January 1, 2023
Revised April 28, 2023
Accepted May 17, 2023
Available online July 1, 2023

Keywords:

Vegetable oil
Magnetic fields
Droplet combustion
Flame characteristics
Flame evolution

1. INTRODUCTION

Increases in population, economy, and the transportation industry escalate the demand for energy, causing the availability of petroleum fuel to run out in the future (Maneechakr & Karnjanakom, 2019). Meanwhile, diesel fuel in high quantities is required for the compression ignition engines of vehicles, despite emitting a lot of harmful emissions to human health and the environment (Saravanan et al., 2020). To overcome this problem, the development of environmentally friendly fuels and new renewable energy for compression ignition engines is extremely necessary (Ooi et al., 2019). Vegetable oils can be processed to become an alternative renewable energy reserve to replace fossil fuels. However, they cannot be used directly in compression ignition engines due to their high viscosity and flash point (Yilmaz et al., 2018), difficulty to burn, imperfect atomization, low evaporation rate, shortening the life of other fuel system components (Mat et al., 2019), and incomplete combustion which results in carbon deposits in the combustion chambers (Mat et al., 2018) and shortens the life of the fuel filter (Yilmaz & Vigil, 2014).

Biodiesel is produced from vegetable oil trough esterification, transesterification, hydrogenation, and catalytic cracking (Zhang & Wu, 2015) by separating glycerol from fatty acids. Efforts to reduce the viscosity of vegetable oils are made by preheating, mixing, and using by microemulsion method (Qi et al., 2013). In the last few decades, studies on mixing vegetable oils with diesel, alcohol, and alcohol-diesel have shown a decrease in viscosity, making it similar to diesel fuel. Numerous studies have investigated vegetable oil-diesel fuel mixtures with different percentage ratios (Agarwal & Dhar, 2013).

Nomenclature

B	biodiesel	Ni-Cr	Nickel-Chromium
fps	frames per second	N-S	North-South
JPG	Joint Photographic Group	Pt	platina
N-N	North-North	Rh	rhodium

It was found that a mixture of 20% vegetable oil and 80% diesel fuel can be used in diesel engines without modifications. However, this mixture still contains fossil fuels as its main constituent (Singh et al., 2016).

Several studies have been done on the combustion of olive oil and its derivatives. Olive oil is one of the most promising substances for use as a substitute for fossil fuels, but has limitations due to low thermal efficiency (Christoforou & Fokaides, 2016). Hasan et al. (2017) investigated the effects of mixing olive oil with gas oil and kerosene from hydrocarbon fuels and found that all pollutants had a lower emission percentage when using olive oil mixed with the additions of 5%, 10%, and 15%. The mixture of olive oil and gas oil resulted in a reduction of unburned hydrocarbons (UHC) by 45.63%, soot by 36.48%, carbon monoxide (CO) by 32.24%, and NOx by approximately 39.54%. Meanwhile, the mixture of olive oil and kerosene showed a decrease in UHC of around 48.92% and soot of 42.13%, CO of 37.41%, and nitrogen oxides (NOx) of 42.85%, compared to kerosene emissions.

A feasibility study has also been carried out on an olive oil compression ignition engine (B100) with five variation of rpm (650, 570, 490, 410, 320, and 240 rpm) and obtained an increase in torque of 8.43% and 28.57% greater power than diesel fuel. In addition, olive oil biodiesel fuel showed the lowest specific energy consumption compared to diesel fuel, namely 12.8% and 30%, at low operating cycles (Volpato et al., 2012). Furthermore, the results of an experimental study using olive pomace oil biodiesel in a diesel engine with an engine load of 18.75 Nm found lower thermal efficiency of around 1% to 5%, CO of 37.5%, and soot emissions of 37.5%, as well as higher NOx by 9.5% and higher CO_2 by 41% compared to diesel fuel with an engine load of 11.25 Nm (Uyumaz et al., 2019). Another study analyzed the performances and pollutants of compression ignition engines with various mixture 20, 40, and 60 at full load which resulted in a brake thermal efficiency (BTE) similar to that of diesel, with less CO emissions for all B20, B40, and B60 mixtures but slightly more NOx (Sree et al., 2017).

Despite numerous studies on biodiesels and relevant topics, magnetic ionization of fuel as a new model has not been widely studied. Magnetic fields have been found to have a positive effect on the fuel combustion process (Wahhab et al., 2017) due to changes in some of its physicochemical properties (Espinosa et al., 2016). Several studies have been done using different measurement methods and revealed that the magnetic field influences the behaviors of the flame (Perdana et al., 2021). Magnetic fields can significantly change the structure (Perdana et al., 2020) and temperature of flame (Agarwal et al., 2018; Perdana et al., 2022). In addition, permanent magnetic fields reduce vehicle fuel consumption and exhaust emissions of CO, hydrocarbon (HC), and NOx (Patel et al., 2014). This is in line with the results of another study which placed permanent magnetic fields in fuel lines and found that the magnetic fields improved the properties of the fuel, accelerated the hydrocarbon molecules to atomize, and produced better vehicle emissions (Jain & Deshmukh, 2012).

From the explanation above, all previous studies only examined the performance of internal combustion engines; only a few studies have provided a broader scientific discussion of the flame phenomenon that occurs in combustion. Therefore, more studies are needed to understand this topic better. This present study burned olive oil as an alternative fuel in the combustion chamber and specifically examined how temperatures and directions of the magnetic fields affect the characteristics of droplet combustion, especially in long-term use in power generation equipment.

2. MATERIAL AND METHOD

2.1 Composition of Fatty Acids and Physicochemical Properties of Olive Oils

Olive oils were obtained from the market with physical and chemical properties as shown in Tables 1 and 2.

2.2 Experimental Apparatus

The experimental apparatus shown schematically in Fig. 1 is used to test the characteristics of the olive oil droplet combustion which are affected by temperature variations of 40°C, 50°C, and 60°C, as well as directions of the magnetic fields of repulse or north- north (N-N) and attractive or north-south (N-S) in the combustion chamber as presented in Fig. 2. Hot air in the combustion chamber is generated by the air heater placed in the air duct before

Table 1 Physical properties of olive oil

Vegetable oil	Physical properties			References
Olive oil	Density (g/cm^3)	15°C	0.917	(Mawatari et al., 2013)
	Kinematic Viscosity (mm^2/s)	40°C	38.7	
		100°C	8.28	
	Flash Point (°C)		285	(Kumar et al., 2014)
	Fire Point (°C)		310	
	Heat of Combustion $\Delta H°_C$ (kJ/g)		43.45	(Villot et al., 2019)

Table 2 Chemical properties of olive oil

Fatty acid		Structure	Value (%)	References
Saturated fatty acids	Myristic	C14:0	0.01	(Guo et al., 2017)
	Palmitoleic	C16:1	1.15	
	Palmitic	C16:1	12.09	
	Margaroleic	C17:1	0.1	
	Margaric	C17:0	0.05	
	Stearic	C18:0	3.01	
Unsaturated fatty acids	Oleic	C18:1	72.77	
	Linoleic	C18:2	9.47	
	Linolenic	C18:3	0.6	
	Arachidic	C20:0	0.36	
	Eicosenoic	C20:1	0.23	
	Behenic	C22:0	0.11	
	Lignoceric	C24:0	0.05	

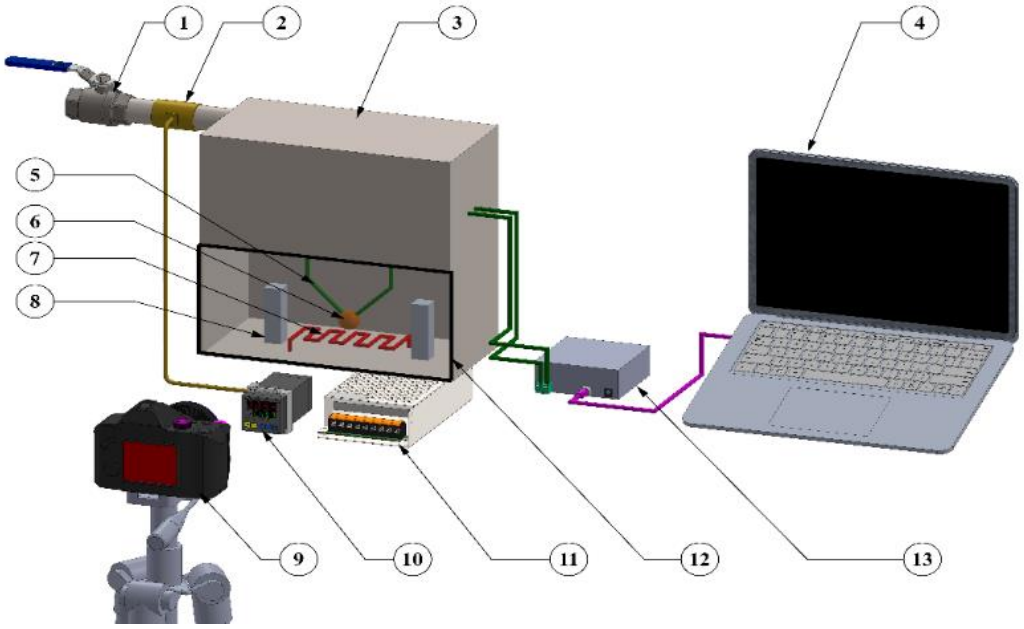

Fig. 1. Experimental apparatus; (1) air intake valve, (2) air heater, (3) temperature chamber, (4) laptop, (5) thermocouple, (6) droplet, (7) electrical heater, (8) permanent magnet, (9) high-speed camera, (10) temperature controller, (11) power supply, (12) quartz glass window on chamber, (13) data logger.

the combustion chamber. The droplet was kept constant at about 0.3 millimeters (mm) in diameter and placed at a type K thermocouple junction made of Pt/Rh13% with a diameter of 0.1 mm serving as a buffer for the droplets and to measure the temperature of the flame. Temperature data began to be collected when the electric heater was turned on and then recorded by the Arduino UNO R3 Atmega 328 data logger at a frequency of 0.01 Hz which was connected to a laptop. The thermocouple was placed at a 10 mm gap between 2 neodymium permanent magnet bars as displayed in Fig. 2. Each magnet bar has dimensions of 40 x 25 x 10 mm and is plated with grade N45 nickel with an intensity of 11000 gauss, and is put in a holder made of aluminum plate. Droplet ignition was done using a heating wire 3 mm below the droplet. The heater is made of nickel-chromium (Ni-Cr) material, with a diameter of 0.7 mm, a length of 30 mm, a voltage of 12, and a current of 5 amperes. The thermocouple junction was connected to the data logger which recorded the temperature of the flame from its ignition to its extinction. Data collected in this study included flame evolution, temperature, height, and ignition delay time. The experiment was performed with ten replications in all cases with stable treatment conditions.

2.3 Data Acquisition

Accuracy of thermocouple is specified at ±8 LSB at operating point of Vcc=3.3V, 0°C to 700°C, with chip at 25°C; 8 LSB means 8 counts, each of which is the range of 1024°C divided by 212°C, equaling 0.25°C per count.

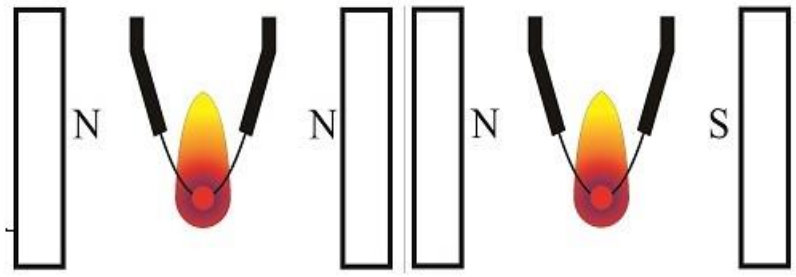

(a) (b)

Fig. 2. Directions of the magnetic fields: (a) repulsive magnetic field (N-N); (b) attractive magnetic field.

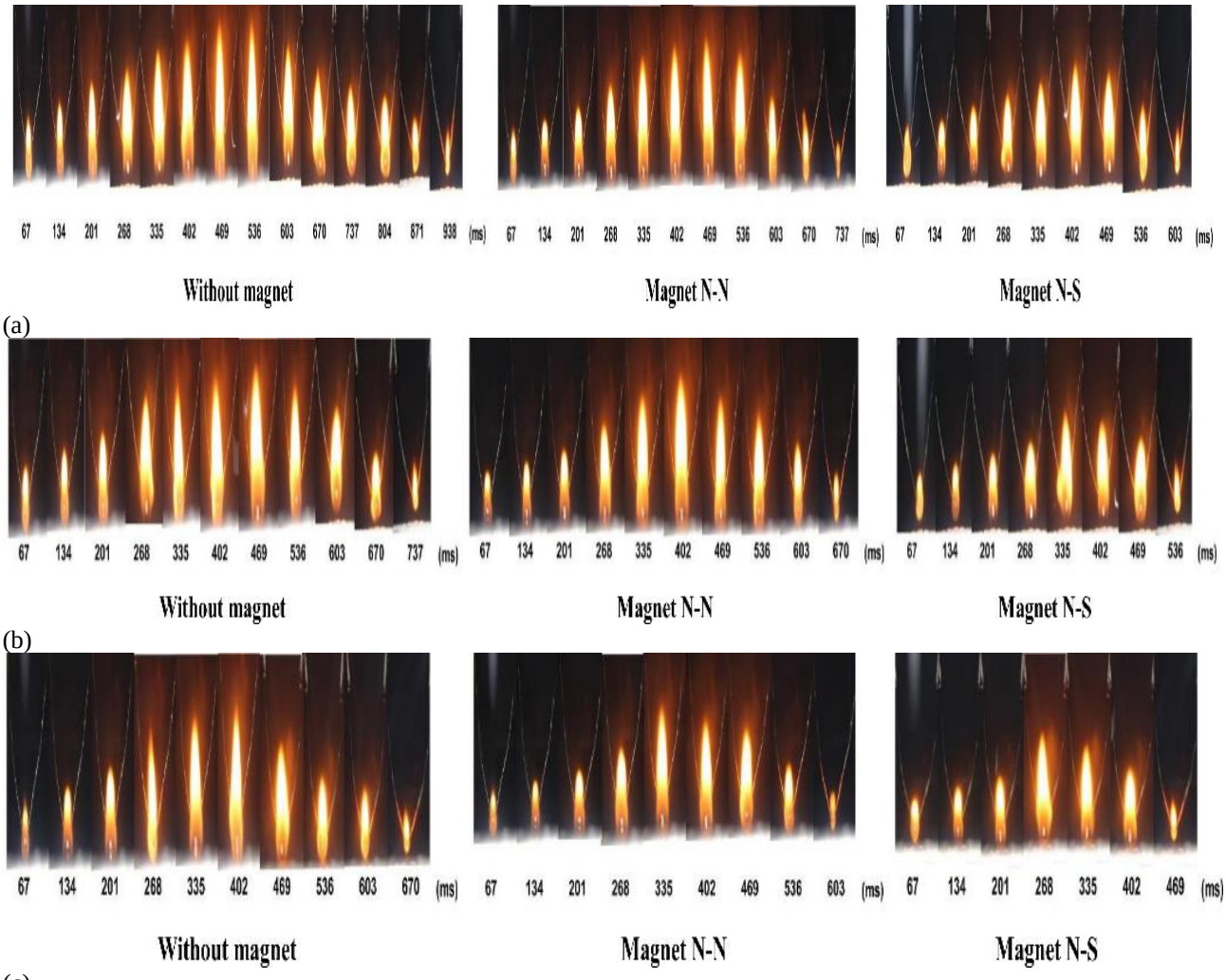

Fig. 3. Flame evolution and shape for evolution time in various directions of the magnetic fields and temperatures of (a) 40°C, (b) 50°C, and (c) 60°C.

Therefore, ±8 LSB means ±2°C. With an offset error of ±3°C from cold junction compensation, the total error is ±5°C. Visualization of the flame was taken starting from the ignition of the flame until its extinction using a 120 frame per second (fps) Fuji ZR high-speed camera placed 20 centimeter (cm) away from the droplet. The collected data were then processed with a free video converter into joint photographic group (JPG) and Image J files, while the evolution time and height of the flame were measured using Corel Draw software.

3. RESULTS AND DISCUSSION

3. 1 Flame Evolution and Shape

As seen in Fig. 3, the flame is slimmer in the combustion chamber without a magnetic field, compared to those of combustion chambers with repulsive (N-N) and attractive (N-S) magnetic fields. Without a magnetic field, the evolution time of the flame was 938 milliseconds (ms) at an initial temperature of 40°C, 737 ms at 50°C, and 670 ms at 60°C. Both magnetic fields, especially the attractive

(N-S) one, have a significant influence on flame evolution and shape. As shown in Fig. 3, the attractive magnetic field (N-S) with a combustion chamber temperature of 60°C produced a shorter evolution time of 469 ms, followed by an evolution time of 536 ms at 50°C and the longest evolution time of 603 ms at 40°C. Meanwhile, for the repulsive magnetic field (N-N), the evolution time and shape of the flame are similar to those of combustion chamber without a magnetic field, i.e., 737 ms at 40°C, 670 ms at 50°C, and 603 ms at 60°C. Furthermore, the attractive magnetic field (N-S) also affects the shape of the flame, where the flame is relatively spherical. This was possibly generated as a result of an explosion due to a significant difference between the temperatures of the droplet and the surrounding environment. With the addition of a magnetic field, this explosion becomes more intense because water (H_2O) and oxygen (O_2) molecules collide, causing the H_2O molecules to break apart faster and each molecule is pulled out of the combustion reaction zone. When it explodes, the fuel vapor in the bubbles does not have enough time to disperse and react quickly, resulting in a round flame (Gamayel et al., 2020).

When the temperature increases, the combustion chamber with an attractive magnetic field (N-S) produces micro-explosions, compared to those with a repulsive magnetic field (N-N) and without a magnetic field. The vapor eruption of a smaller amount of saturated fatty acids leads to micro-explosions at lower oil temperatures. Conversely, micro-explosions at higher oil temperatures are associated with the breakdown of low-viscosity unsaturated fatty acids due to eruption of fatty acid vapors. Furthermore, the asymmetry of the flame shape characterizes the explosion in droplet combustion which indicates the amount of energy generated from the combustion. Fig. 3c signifies that rapid combustion process causes a lower flame height.

Strong magnetic field intensity may produce attractive forces between hydrocarbon molecules, hereby breaking them down. The broken hydrocarbons leave maximum space for O_2 molecules to combine with the fuel molecules. As a result, the hydrocarbon molecules become more reactive to O_2, making them more flammable.

Magnetic fields affect the speed and dimensions of the combustion, with different direction of the magnetic fields having different effect on the speed of the combustion. With this regards, the repulsive magnetic field (N-N) has less influence than the attractive magnetic field (N-S); it produces a lower speed of flame. This is because N-S pumps more heat brought by H_2O to the flame, while N-N pumps the heat-carrying H_2O out of the flame.

3.2. Flame Temperature

Figure 4 displays the temperature of droplet combustion in the combustion chamber with various directions of the magnetic fields and temperatures of 40°C, 50°C, and 60°C and. At a temperature of 40°C, the combustion chamber with an attractive magnetic field (N-S) produced the highest temperature of 799.94°C at 402 ms, followed by those with a repulsive magnetic field (N-N) and without a magnetic field, which generated 691.67°C at 469 ms and 673.25°C at 536 ms, respectively, as seen in Fig. 4a. Meanwhile, at a temperature of 50°C, the lowest flame temperature of 726.21°C at 469 ms occurs in the combustion chamber without a magnetic field and the highest of 920.25°C was in the combustion chamber with an attractive magnetic field (N-S), whereas the one with a repulsive magnetic field (N-N) produced a flame temperature of 764.5°C (See Fig. 4b). Fig. 4c shows the combustion chamber at a temperature of 60°C, with the highest flame temperature of 879.5°C at 268 ms being in the one with an attractive magnetic field (N-S), followed by those with a repulsive magnetic field (N-N) and without a magnetic field, namely 815.5°C at 335 ms and 794.55°C at 402 ms, respectively.

Figures 4a-4c show that the flame temperature produced is the lowest in combustion chamber without a magnetic field than in those with repulsive (N-N) and attractive (N-S) magnetic fields. The flame temperature in the combustion chamber with repulsive magnetic field (N-N) is almost the same as that without a magnetic field, while the highest flame temperature occurs in the combustion chamber with attractive magnetic field (N-S). This proves that the direction of the magnetic field affects flame temperature in droplet combustion; the greater the intensity of the magnetic field, the higher the flame temperature produced. The rich O_2 around the flame causes combustion to occur ideally, with the maximum flame temperature occurs around the middle of the combustion process. This is made possible by the transition of burning droplets from unsaturated fatty acids, which begin to run out, towards saturated fatty acids, which begin to burn, causing a huge explosion.

The high flame temperature of the olive oil droplet combustion indicates the power generated by the combustion. Magnetic fields interfere with the movement of electrons in the fatty acid molecules, causing them to move out of their orbits. When given heat, the fatty acid bonds weaken and move away from each other, making them break more quickly. However, the electrons that come out of their orbits do not result in the fatty acids only having positively charged protons. During combustion, oxygen has a high electronegativity to attract electrons to move to negatively-charged oxygen. When the negatively-charged oxygen reacts to the positively-charged fatty acids, it creates a massive attraction. Such attractive force causes collisions between molecules, accelerating the combustion reaction so that the maximum combustion temperature increases (Fig. 4c).

3.3 Flame Height

The difference in the height of the flame from droplet combustion, which is affected by various temperatures and directions of the magnetic field in a combustion chamber, is shown in Fig. 5. Figure 5a shows the flame height at the combustion chamber temperature of 40°C, with the highest being 7.36 mm at 536 ms in the combustion chamber without a magnetic field.

Meanwhile, the highest flame height in the combustion chamber with a repulsive magnetic field (N-N) was 6.96 mm, whereas that of the combustion chamber with an

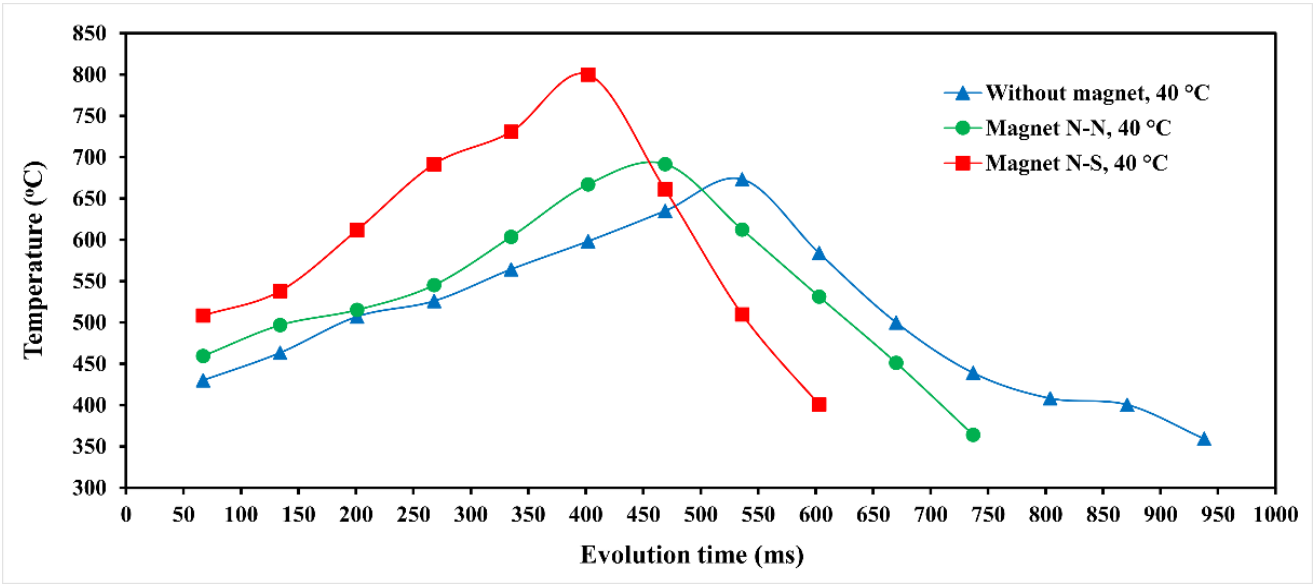

(a)

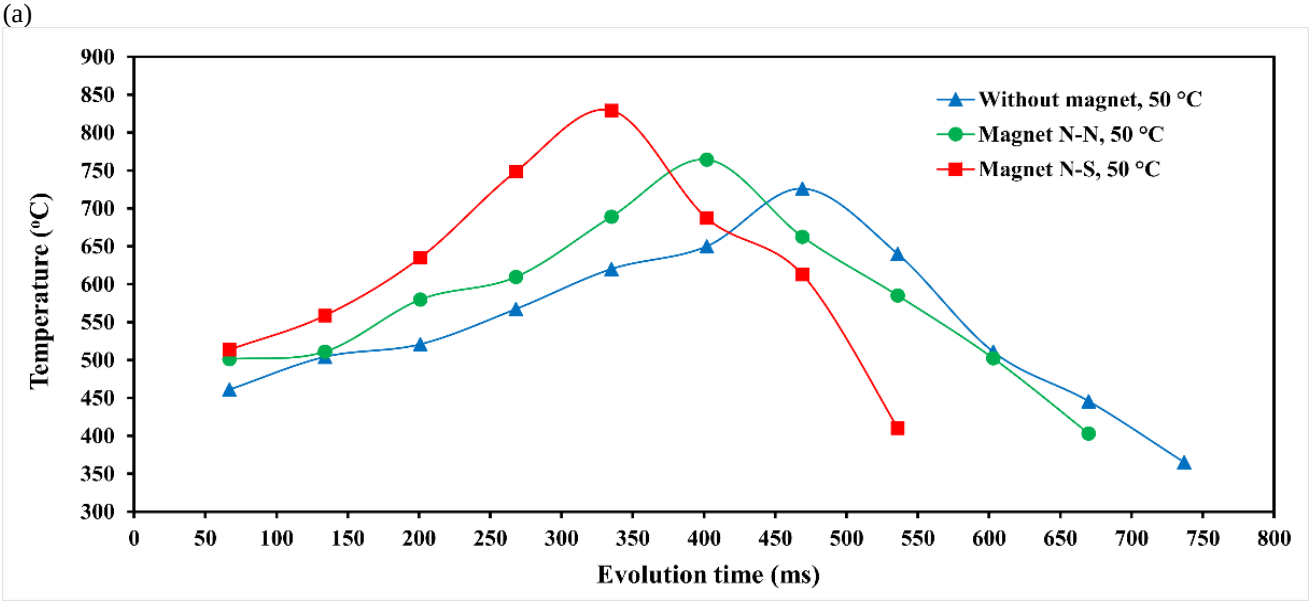

(b)

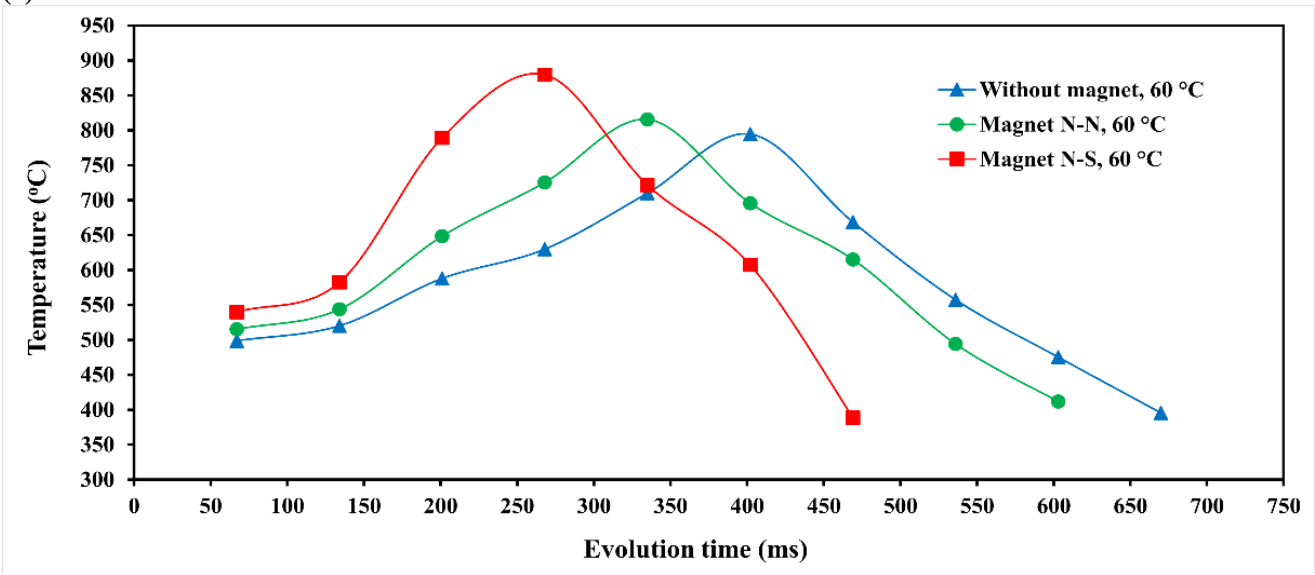

(c)

Fig. 4. Flame temperature for evolution time in various directions of the magnetic fields and temperatures in the combustion chamber of (a) 40°C, (b) 50°C, and (c) 60°C.

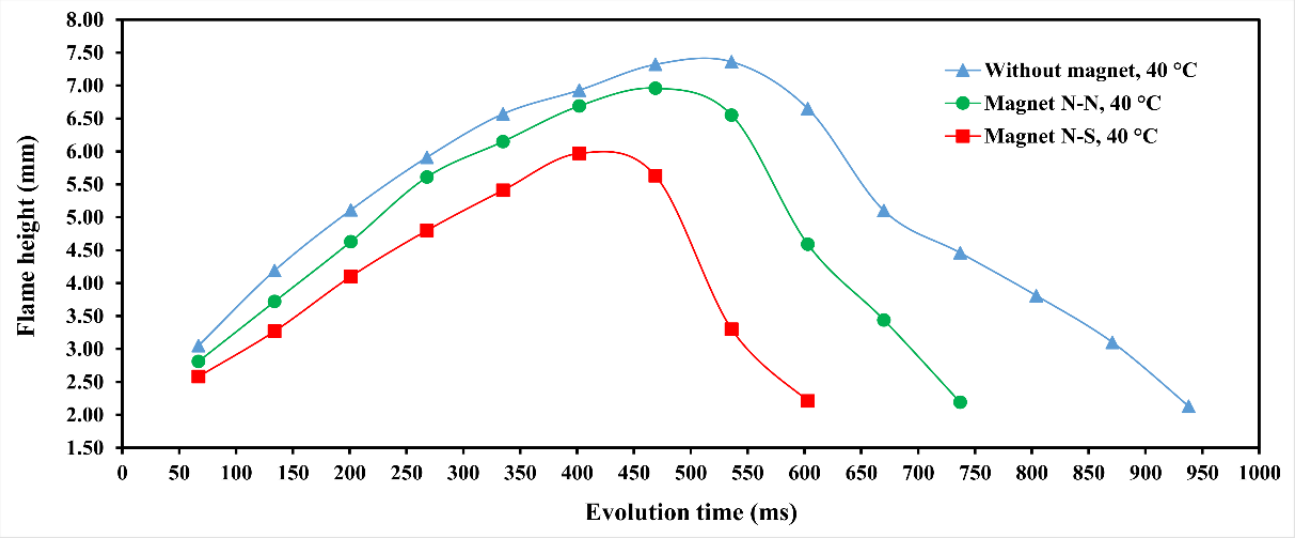

(a)

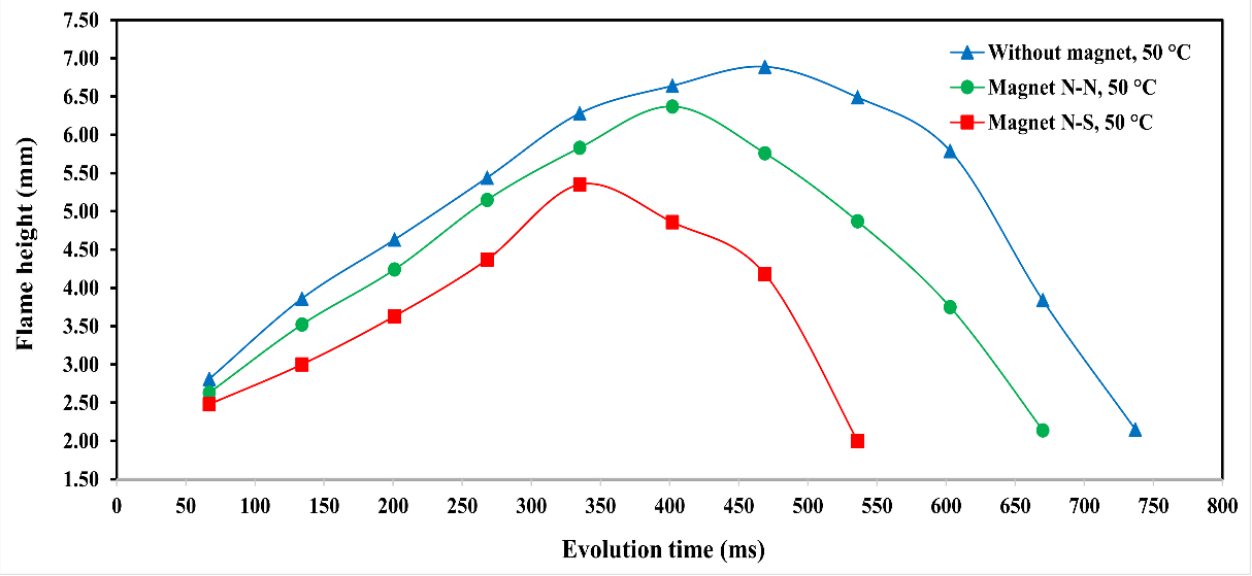

(b)

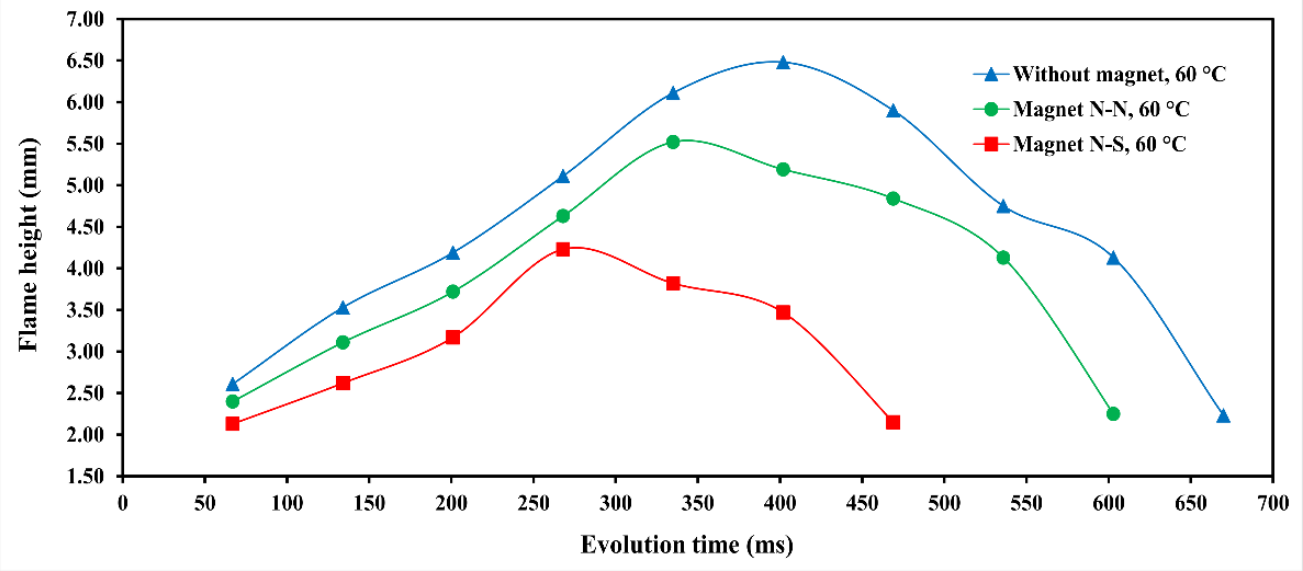

(c)

Fig. 5. Flame height for evolution time in various directions of the magnetic fields and temperatures in the combustion chamber of (a) 40°C, (b) 50°C, and (c) 60°C.

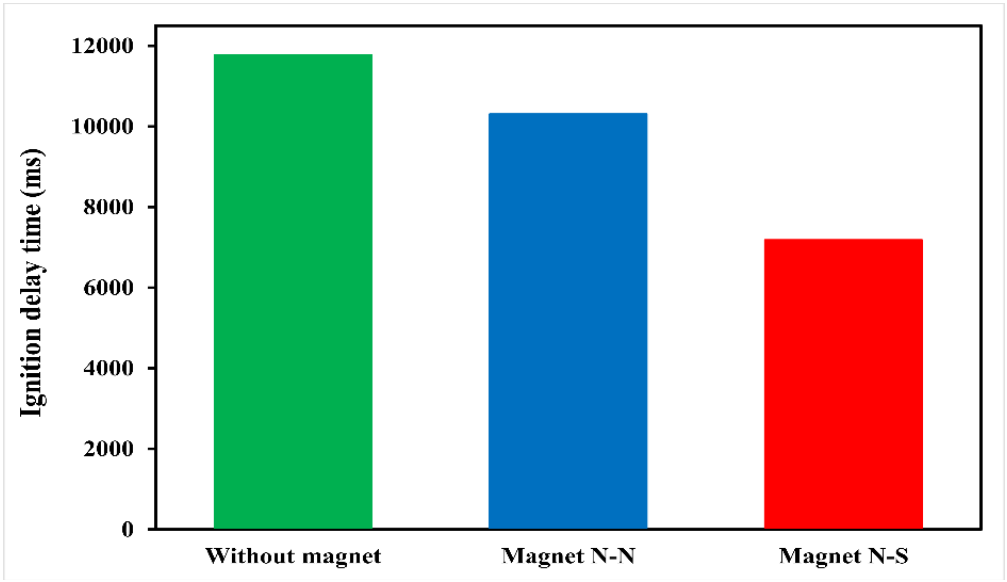

(a)

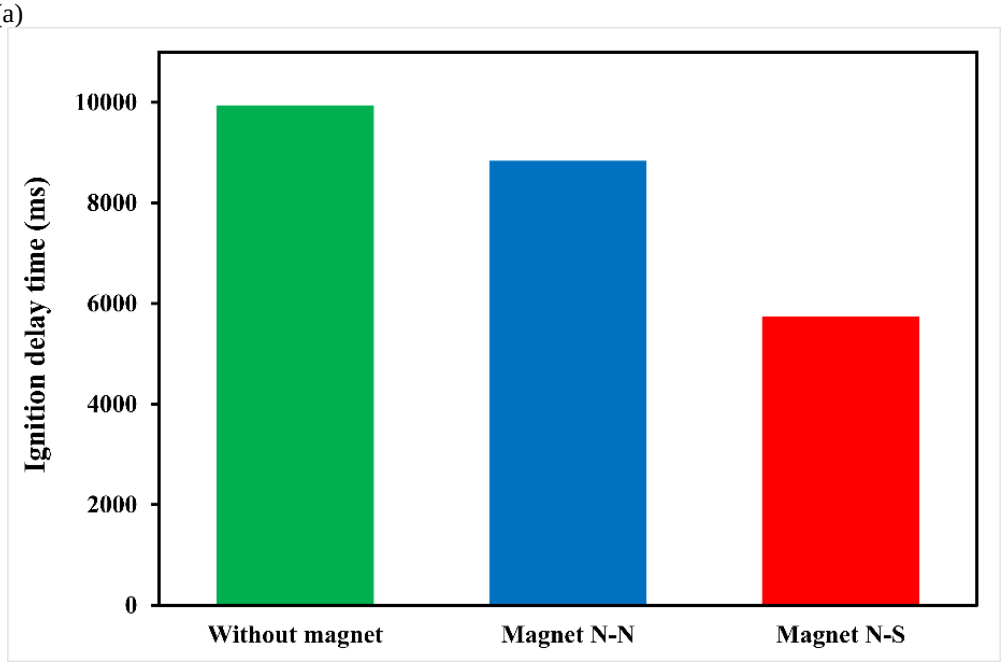

(b)

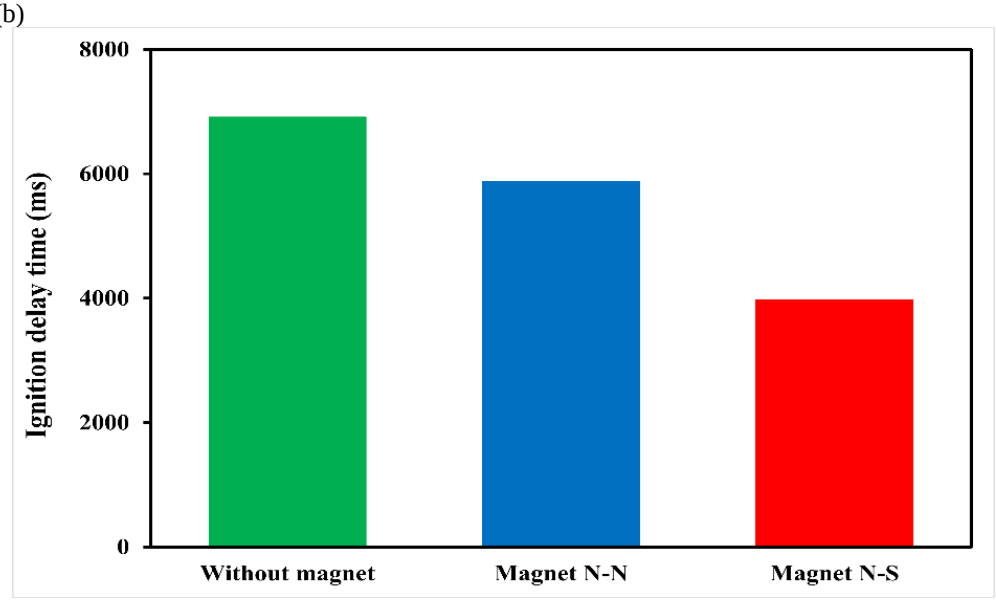

(c)

Fig. 6. Ignition delay time as the evolution time in various directions of the magnetic fields and temperatures in the combustion chamber of (a) 40°C, (b) 50°C, and (c) 60°C.

attractive magnetic field (N-S) was 5.97 mm at 420 ms. As presented in Fig. 5b, at the combustion chamber temperature of 50°C the combustion chamber with an attractive magnetic field (N-S) produces the lowest flame height of 5.35 mm at 335 ms, followed by 6.89 mm at 469 ms in the combustion chamber without a magnetic field and 6.37 mm at 402 ms in the combustion chamber with a repulsive magnetic field (N-N). At a temperature of 60°C, the three combustion chambers have the lowest flame height and the shortest evolution time, compared to the other temperatures. The highest flame of 6.48 mm occurred in the combustion chamber without a magnetic, followed by 5.52 mm (N-N) and 4.23 mm (N-S), with varying evolution times (See Fig. 5c).

The dimensions of the flame slowly increase during the early combustion period. This is related to the fuel-air accumulation which diffuses around the droplets. One of the causes of the difference in flame height is the high combustion chamber temperature which leads to a decrease in viscosity, thus making the combustion process take place quickly. The higher the temperature in the combustion chamber, the more vapors generated through the evaporation of droplet surface diffuse into the air, causing the flame height to be shorter. It is because. In addition, the size of the flame decreases drastically once it reaches its maximum height. The highest flame indicates an extremely unreactive combustion process; the combustion is not complete as some portion of the fuel is not burned. In this experiment, the attractive magnetic field (N-S) was found to pull O_2 from the air around the flame. This pushes out H_2O from the combustion, thus accelerating the combustion reaction with the fuel (Perdana et al., 2020). Oxygen is attracted by the N-S magnetic field and then flows to the base of the flame from both sides. This flow increases the concentration of oxygen and fuel molecules in the vicinity of the reaction zone, causing more reactive and brief combustion and contributing to an increase in flame height. The stronger the magnetic field intensity, the shorter the flame height.

3.4 Ignition Delay Time

Figure 6 displays the ignition delay time of the flame in various temperatures and directions of the magnetic fields in the combustion chambers. At a temperature of 40°C, the combustion chamber without a magnetic field produces the longest ignition delay time of around 11775 ms, followed by an ignition delay time of of 10310 ms in the combustion chamber with a repulsive magnetic field (N-N). Meanwhile, the shortest ignition delay time of 7187 ms occurs in the combustion chamber with an attractive magnetic field (N-S), as shown in Fig. 6a. Fig. 6b signifies that the combustion chamber with an attractive magnetic field (N-S) generates the shortest ignition delay time of 5725 ms, followed by an ignition delay time of 8819 ms in the combustion chamber with a repulsive magnetic field (N-N), whereas the combustion chamber without a magnetic field has the longest ignition delay time of 9926 ms, at a temperature of 50°C. Furthermore, the shortest ignition delay time in all combustion chambers occurs at a temperature of 60°C, compared to the other temperatures, where the ignition delay times in the combustion chamber with an attractive magnetic field (N-S), with a repulsive magnetic fields (N-N), and without a magnetic field are 3973 ms, 5876 ms, and 6910 ms, respectively.

The temperature in the combustion chamber affects the ignition delay time; the higher the temperature, the shorter the ignition delay time. This causes the viscosity to decrease, thereby increasing the possibility of more micro-explosions and a better combustion process. As seen in Table 2, olive oil has higher unsaturated fatty acids than saturated fatty acids. Vegetable oils start to burn with unsaturated fatty acids, saturated fatty acids, and glycerol (Wardana, 2010). When the temperature of the combustion chamber reaches 60°C, unsaturated fatty acids, mainly oleic and linoleic, begin to form in the evaporation phase before diffusing with the oxidizing agent to form reactants and burn. The shorter evaporation process causes the diffusion of fuel with the oxidizer to occur in a narrow area. A short ignition delay occurs due to several factors. First, an increase in the temperature of the combustion chamber in olive oil droplet combustion accelerates the combustion reaction as the unsaturated fatty acids have a low flash point. Second, the attractive magnetic field (N-S) helps to enhance the atomization process by speeding up the formation of the mixture. Third, the magnetic field creates an electromagnetic force that disturbs the electrons in olive oil so that the activation energy needed to react with fuel and oxygen is reduced, causing the combustion to take place relatively faster.

4. CONCLUSIONS

This experimental study was carried out on olive oil droplet combustion in various temperatures and directions of the magnetic fields in the combustion chamber, with the droplet combustion being observed from the initial formation of the flame to its extinction. The main conclusions that can be drawn from this study are:

1. The magnetic fields with greater intensity make the rotating electrons and protons more energetic and the combustion reaction rate more reactive which results in shorter flame and wider area.
2. The magnetic fields increase the supply of oxygen, and the flow of molecular fuel to the base of the flame becomes more reactive and flammable, causing the temperature to rise.
3. The magnetic fields increase the energy of the intermolecular vibrations, leading to a fast combustion speed and a shorter ignition delay.

ACKNOWLEDGEMENTS

We would like to express our heartfelt gratitude to Ario Rivaldo, Lukman Hakim, and Ahmad Nuril Mubin for collecting the experimental data, as well as to Maarif Hasyim Latif University, Sidoarjo for funding this study.

CONFLICT OF INTEREST

The authors declare that they have no conflict of interest in relation to this research, whether financial, personal,

authorship or otherwise, that could affect the research and its results presented in this paper.

AUTHORS CONTRIBUTION

D. Perdana: conceptualization; lead data curation; lead formal analysis; funding acquisition; methodology; lead project administration; lead resources; supervision; lead validation; lead visualization; lead writing – original draft; lead writing – review & editing. M. Hanifudin: supporting data curation; supporting investigation; supporting resources; lead software; supporting visualization. M. K. Rosidin: supporting investigation; supporting resources; supporting software; supporting visualization; supporting writing – original draft; supporting writing – review & editing. W. A. Winarko: supporting data curation; supporting formal analysis; lead investigation; supporting project administration; supporting resources; supporting validation; supporting writing – review & editing

REFERENCES

Agarwal, A. K., & Dhar, A. (2013). Experimental investigations of performance, emission and combustion characteristics of karanja oil blends fuelled DICI engine. *Renewable Energy*, 52, 283–291. https://doi.org/10.1016/j.renene.2012.10.015

Agarwal, S., Kumar, V., & Shakher, C. (2018). Temperature measurement of wick stabilized micro diffusion flame under the influence of magnetic field using digital holographic interferometry. *Optics and Lasers in Engineering*, 102, 161–169. https://doi.org/10.1016/j.optlaseng.2017.10.019

Christoforou, E., & Fokaides, P. A. (2016). A Review of olive mill solid wastes to energy utilization techniques. *Waste Management*, 49, 346–363. https://doi.org/10.1016/j.wasman.2016.01.012

Espinosa, E. A. M., Rodríguez, R. P., Sierens, R., & Verhelst, S. (2016). Emulsification of waste cooking oils and fatty acid distillates as diesel engine fuels: an attractive alternative. *International Journal of Sustainable Energy Planning and Management*, 9, 3–16. https://doi.org/10.5278/ijsepm.2016.9.2

Gamayel, A., Mohammed, M. N., Al-Zubaidi, S., & Yusuf, E. (2020). Effect of clove oil in droplet combustion of crude jatropha oil. *International Journal of Advanced Science and Technology*, 29 (5s), 1564–1571. http://sersc.org/journals/index.php/IJAST/article/view/8272

Guo, Z., Jia, X., Zheng, Z., Lu, X., Zheng, Y., Zheng, B., & Xiao, J. (2017). Chemical composition and nutritional function of olive (Olea europaea L.): a review. *Phytochemistry Reviews*, 17(5), 1091–1110. https://doi.org/10.1007/s11101-017-9526-0

Hasan, A. K. M., Jawad, A. S. M., & Ekaab, N. S. (2017). Experimental stady of using olive oil and biodiesel on pollutants emissions in the continuous combustion chamber. *Journal of Engineering and Sustainable Development*, 21(02), 192–204. https://jeasd.uomustansiriyah.edu.iq/index.php/jeasd/article/view/599

Jain, S., & Deshmukh, S. (2012). Experimental investigation of magnetic fuel conditioner (MFC) in IC engine. *IOSR Journal of Engineering*, 2(7), 27–31. http://www.iosrjen.org/Papers/vol2_issue7%20(part-1)/E0272731.pdf

Kumar, S. S., Iruthayarajan, M. W., & Bakrutheen, M. (2014, November). Analysis of vegetable liquid insulating medium for applications in high voltage transformers. In *Proceedings of International Conference on Science, Engineering and Management Research, Chennai, India*. https://ieeexplore.ieee.org/document/7043606

Maneechakr, P., & Karnjanakom, S. (2019). A combination of 2k factorial with box-behnken designs for FAME production via methanolysis of waste cooking palm oil over low-cost catalyst. *Journal of Environmental Chemical Engineering*, 7(6), 103389. https://doi.org/10.1016/j.jece.2019.103389

Mat, S. C., Idroas, M. Y., Hamid, M. F., & Zainal, Z. A. (2018). Performance and emissions of straight vegetable oils and its blends as a fuel in diesel engine: *A review. Renewable and Sustainable Energy Reviews*, 82, 808–823. https://doi.org/10.1016/j.rser.2017.09.080

Mat, S. C., Idroas, M. Y., Teoh, Y. H., & Hamid, M. F. (2019). Optimisation of viscosity and density of refined palm oil-melaleuca cajuputi oil binary blends using mixture design method. *Renewable Energy*, 133, 393–400. https://doi.org/10.1016/j.renene.2018.10.017

Mawatari, T., Fukuda, R., Mori, H., Mia, S., & Ohno, N. (2013). High pressure rheology of environmentally friendly vegetable oils. *Tribology Letters*, 51(2), 273–280. https://doi.org/10.1007/s11249-013-0180-4

Ooi, J. B., Yap, J. H., Tran, M. V., & Leong, J. C. K. (2019). Experimental investigation on the droplet burning behavior of diesel - Palm biodiesel blends. *Energy Fuels*, 33(11). 11804–11811. https://doi.org/10.1021/acs.energyfuels.9b02259

Patel, P. M., Rathod, G. P., & Patel, T. M. (2014). Effect of magnetic field on performance and emission of single cylinder four stroke diesel engine. *IOSR Journal of Engineering*, 4(5), 28–34. http://www.iosrjen.org/Papers/vol4_issue5%20(part-5)/F04552834.pdf

Perdana, D., Yuliati, L., Hamidi, N., & Wardana, I. N. G. (2020). The role of magnetic field orientation in vegetable oil premixed combustion. *Journal of Combustion*, 2020, 1–11. https://doi.org/10.1155/2020/2145353

Perdana, D., Adiwidodo, S., Choifin, M., & Winarko, W. A. (2021). The effect of magnetic field variations in a mixture of coconut oil and jatropha on flame stability and characteristics on the premixed combustion. *EUREKA: Physics and Engineering*, 2021(5), 13–22. https://doi.org/10.21303/2461-4262.2021.001996

Perdana, D., Adiwidodo, S., Subagyo S. & Winarko, W. A. (2022). The role of perforated plate and orientation of the magnetic fields on coconut oil premixed combustion. *INMATEH - Agricultural Engineering*, 67(2), 77–84. https://doi.org/10.35633/inmateh-67-07

Qi, D. H., Bae, C., Feng, Y. M., Jia, C. C., & Bian, Y. Z. (2013). Combustion and emission characteristics of a direct injection compression ignition engine using rapeseed oil based microemulsions. *Fuel*, 107, 570–577. https://doi.org/10.1016/j.fuel.2013.01.046

Saravanan, P., Kumar, N. M., Ettappan, M., Dhanagopal, R., & Vishnupriyan, J. (2020). Effect of exhaust gas re-circulation on performance, emission and combustion characteristics of ethanol-fueled diesel engine. *Case Studies in Thermal Engineering*, 20, 100643. https://doi.org/10.1016/j.csite.2020.100643

Singh, P., Varun, V., Chauhan, S. R., & Kumar, N. (2016). A Review on methodology for complete elimination of diesel from ci engines using mixed feedstock. *Renewable and Sustainable Energy Reviews*, 57, 1110–1125. https://doi.org/10.1016/j.rser.2015.12.090

Sree, S. N., Kumar, K. S., & Nidumolu, E. P. (2017). Experimental investigation on CI engine fuelled with the blends of olive oil methyl ester and diesel. *International Journal of Mechanical Engineering and Technology*, 8(7), 125–132. https://iaeme.com/MasterAdmin/Journal_uploads/IJMET/VOLUME_8_ISSUE_7/IJMET_08_07_015.pdf

Uyumaz, A., Aksoy, F., Akay, F., Baydır, Ş. A., Solmaz, H., Yılmaz, E., Aydoğan, B., & Calam, A. (2019). An experimental investigation on the effects of waste olive oil biodiesel on combustion, engine performance and exhaust emissions. *International Journal of Automotive Engineering and Technologies*, 8(3), 103–116. https://doi.org/10.18245/ijaet.578227

Villot, C., Howard, M. E., & Kittredge, K. W. (2019). Comparison of various feedstocks for the microwave-assisted synthesis of biodiesel. *American Journal of Organic Chemistry*, 9(2), 25–27. http://article.sapub.org/10.5923.j.ajoc.20190902.01.html

Volpato, C. E. S., Do, A., Conde, P., Barbosa, J. A. & Salvador, N. (2012). Performance of cycle diesel engine using biodiesel of olive oil (B100). *Ciência e Agrotecnologia*, 36(3), 348–353. https://doi.org/10.1590/S1413-70542012000300011

Wahhab, H. A. A., Al-Kayiem, H. H., Aziz, A. A. R., & Nasif, M. S. (2017). Survey of invest fuel magnetization in developing internal combustion engine characteristics. *Renewable and Sustainable Energy Reviews*, 79, 1392–1399. http://doi.org/10.1016/j.fuel.2009.07.002

Wardana, I. N. G. (2010). Combustion characteristics of jatropha oil droplet at various oil temperatures. *Fuel*, 89(3), 659–664. https://doi.org/10.1016/j.fuel.2014.01.075

Yilmaz, N., & Vigil, F. M. (2014). Potential use of a blend of diesel, biodiesel, alcohols and vegetable oil in compression ignition engines. *Fuel*, 124, 168–172. https://doi.org/10.1016/j.fuel.2017.10.050

Yilmaz, N., Atmanli, A., & Vigil, F. M. (2018). Quaternary blends of diesel, biodiesel, higher alcohols and vegetable oil in a compression ignition engine. *Fuel*, 212, 462–469. https://doi.org/10.1016/j.fuel.2017.10.050

Zhang, M., & Wu, H. (2015). Effect of major impurities in crude glycerol on solubility and properties of glycerol/methanol/bio-oil blends. *Fuel*, 159, 118–127. https://doi.org/10.1016/j.fuel.2015.06.062